

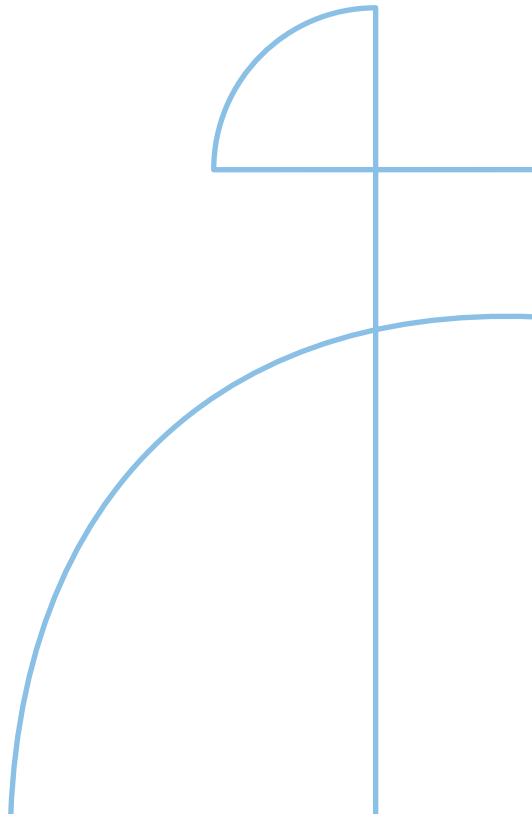


Licentiate Thesis in Aerospace Engineering

# Non-linear structural phenomena influencing flutter performance

ANDERS ELLMO

KTH ROYAL INSTITUTE OF TECHNOLOGY



# Non-linear structural phenomena influencing flutter performance

ANDERS ELLMO

Academic Dissertation which, with due permission of the KTH Royal Institute of Technology, is submitted for public defence for the Degree of Licentiate of Engineering on Friday the 29th of May 2026, at 10:15 a.m. in Meetingroom Freja, Teknikringen 8, Stockholm.

Licentiate Thesis in Aerospace Engineering  
KTH Royal Institute of Technology  
Stockholm, Sweden 2026

© Anders Ellmo  
© Andreas Linderholt, Paper C

TRITA-SCI-FOU-2026:10  
ISBN 978-91-8106-584-8

Printed by: Universitetservice US-AB, Sweden 2026

*Dedicated to my wife and daughters, without whom none of this matters.*



# Abstract

This thesis explores the effect of local non-linear phenomena on a structure that can otherwise be described linearly with a high degree of accuracy, with the focus on fuel sloshing in external stores. While it is possible to make high fidelity simulations of these phenomena, they are complex enough that it is not possible in a production environment where thousands of analyses are made.

Experimental modal analysis of multiple sets of composite wings show manufacturing induced asymmetries, with a significant frequency shift observed in the first bending mode between the left and right wings of one set. These variations caused nominal symmetric and anti-symmetric mode shapes to shift into single wing dominated modes. Tests using a wing-fuel tank system demonstrated that liquid-filled configurations exhibit distinct dynamic behaviors compared to rigid-mass equivalents. At a 50% fill level, a store sway structural mode present in the dry configuration was found to dissipate in the wet configuration. Additionally, the liquid-filled stores were subject to frequency shifts in torsional modes and an increase in overall structural damping. Excitation using robotic motion was evaluated using the same sloshing tank attached to a six-degrees-of-freedom industrial robot, with a focus on achieving chaotic fluid motion. It is shown to be a valid alternative to traditional excitation schemes.

Numerical simulations using individually updated finite element models showed a substantial variation in critical flutter speeds. Configurations utilizing liquid-filled tanks demonstrated higher critical flutter velocities than rigid-filled counterparts due to increased frequency separation between fundamental wing bending and torsion modes. The results indicate that linear models approximating fuel as a frozen mass can lead to an underestimation of critical dynamic pressure. Experimental validation remain essential for ensuring the robustness of analytical flutter predictions.

## **Keywords**

structural dynamics, aeroelasticity, sloshing



# Sammanfattning

Denna avhandling utforskar effekten av lokala icke-linjära fenomen på en struktur som i övrigt kan beskrivas linjärt med hög noggrannhet, med fokus på bränsleskvalp i externa laster. Trots att högupplösta simuleringar av dessa fenomen är möjliga, är de så komplexa att det inte är möjligt att använda dessa i en skarp produktutvecklingsmiljö där tusentals analyser genomförs.

Experimentell modalanalys av flera uppsättningar kompositvingar uppvisar tillverkningsinducerade asymmetrier, med en signifikant frekvensförskjutning för första böjmoden mellan vingarna i en uppsättning. Dessa variationer orsakade att nominellt symmetriska och antisymmetriska modformer skiftade till moder dominerade av en vinge i taget. Tester av ett vingsystem med bränsletank visade att vätskefyllda konfigurationer uppvisar distinkta beteenden jämfört med motsvarigheter fyllda med stel massa. Vid en fyllnadsgrad på 50 % i den våta konfigurationen försvann en strukturell mod för sidrörelse (store sway), som fanns i den torra konfigurationen. Dessutom introduceras tydliga frekvensskift och en ökning av strukturell dämpning i torsionsmoder. Excitering med industrirobot utvärderades med samma tank monterad på en robot, med fokus på förmågan att uppnå kaotisk vätskerörelse. Det visas vara ett giltigt alternativ till shakerexcitering.

Numeriska simuleringar med individuellt uppdaterade finita elementmodeller visade på en variation i kritiska fladderhastigheter. Konfigurationer med vätskefyllda tankar uppvisade generellt högre kritiskt dynamiskt tryck än motsvarigheter med stel massa, på grund av en ökad frekvensseparation mellan vingens fundamentala böj- och torsionsmoder. Resultaten indikerar att linjära modeller som approximerar bränsle som en frusen massa, kan leda till en underskattning av kritiskt dynamiskt tryck. Experimentell validering av strukturdynamiska egenskaper är avgörande för att säkerställa robustheten i analytiska fladderprediktioner.

## **Nyckelord**

strukturdynamik, aeroelasticitet, bränsleskvalp



# Acknowledgment

I would like to express my sincere gratitude to Professor Ulf Ringertz for his supervision during this project, with invaluable guidance and support. Thank you Ulf for generously sharing your experience and knowledge with me. Additionally, I would like to thank my manager Pär Gustafsson for his unending enthusiasm, and for making this adventure possible. Thank you also to Professor Andreas Linderholt of Linnaeus University in Växjö for your contributions to the project, for reviewing my work and providing important improvements.

A significant portion of the experimental testing was conducted at the Transonic Dynamics Tunnel at NASA Langley Research Center. I would like to recognize and thank Donald F. Keller, Walter A. Silva, Jennifer L. Pinkerton and Ian M. Giles of the Aeroelasticity Branch for their technical facilitation and support throughout the duration of the activities. Thank you for providing insight in NASA's work and facilities, a fascinating and appreciated experience.

I would also like to express my sincere appreciation to my colleagues, whose discussions and contributions have refined the quality of this work. I am especially grateful to Anders Karlsson for his support and encouragement.

To my family and friends: thank you for believing in me and for your patience while I navigated this chapter. I hope you will still be there when I have to do it again shortly!

This work was partially supported by Nationellt Flygforskningsprogram (NFFP8), funded by Vinnova.

Sincerely,  
Anders Ellmo  
Stockholm, April 30, 2026



## List of included papers

The following list of papers summarizes the contributions of this licentiate thesis to the field of aeroelastics and structural dynamics.

- Paper A** **Ground Vibration Testing and Model Update of a Transonic Flutter Wind Tunnel Model**, A. Ellmo. In Proceedings of the 20th International Forum on Aeroelasticity and Structural Dynamics (IFASD), 2024. Updated version.
- Paper B** **Design and testing of a wing-fuel tank system for fuel-slosh studies**, A. Ellmo. In Proceedings of the 21st International Forum on Aeroelasticity and Structural Dynamics (IFASD), 2026. Accepted for presentation.
- Paper C** **Sloshing tests using a six degree-of-freedom robot**, A. Ellmo and A. Linderholt. In , 2026. Preliminary version.

## Division of work between authors

- Paper C** Ellmo constructed the test object, as well as planned and carried out sloshing tests. Linderholt implemented programming and control of the industrial robot. The paper was written by Ellmo with support from Linderholt.



# Contents

<b>Abstract</b> . . . . .	3
<b>Sammanfattning</b> . . . . .	5
<b>Acknowledgment</b> . . . . .	7
<b>List of included papers</b> . . . . .	9
<b>Division of work between authors</b> . . . . .	9
<b>Contents</b> . . . . .	11
<b>List of Figures</b> . . . . .	13
<b>List of Tables</b> . . . . .	15
<b>I Introduction</b> . . . . .	1
<b>1 Introduction</b> . . . . .	3
1.1 Motivation . . . . .	6
1.2 Research aim and research questions . . . . .	7
1.3 Scope . . . . .	7
<b>2 Background</b> . . . . .	9
2.1 Aeroelasticity . . . . .	9
2.2 Sloshing . . . . .	10
2.3 Sloshing and aeroelasticity . . . . .	15
<b>3 Materials and methods</b> . . . . .	17
3.1 Structural dynamics . . . . .	17
3.2 Aeroelasticity . . . . .	22
<b>4 Results</b> . . . . .	25
<b>5 Conclusions and future work</b> . . . . .	27
5.1 Future Research Directions . . . . .	27
<b>Bibliography</b> . . . . .	29
<b>About the use of generative AI</b> . . . . .	33
<b>II Appended papers</b> . . . . .	35



# List of Figures

1.0.1 JAS 39 Gripen C with an assortment of external stores. Photo by Patrik Skolling Möller. . . . .	3
1.0.2 Ground Vibration Tests have been performed with both fuel-filled drop tanks, and solid equivalent dummies. The tests were done at differing times, and on different aircraft individuals. . .	5
1.0.3 Comparison of the vertical response at a driving point, between a liquid filled drop tank and a dummy drop tank with similar mass properties. . . . .	6
2.1.1 The aeroelastic triangle, adapted from Collar [6]. . . . .	9
2.2.2 The pitch oscillation apparatus used by Widmeyer and Reese [33].	14
3.1.1 Ongoing ground vibration test of a JAS 39 Gripen E aircraft. . .	19
3.1.2 Example of force and response on a simple plate. . . . .	20
3.1.3 Overview of a generic test setup employing shaker excitation. . .	20
3.1.4 Analysis process in experimental modal analysis. . . . .	21



# List of Tables

2.2.1 Fluid properties for JP-8 and tap water. . . . .	13
--	----



# Introduction



# 1 Introduction

Modern aerospace structural design is a delicate balancing act between development cost, delivery speed, and structural performance. For a multi-role fighter like the JAS 39 Gripen, this balance is tested by an almost infinite matrix of altitudes, temperatures, speeds, and maneuvers combined with a vast array of mass loads and external store configurations (Figure 1.0.1).



**Figure 1.0.1:** JAS 39 Gripen C with an assortment of external stores. Photo by Patrik Skolling Möller.

To simplify the latter, the fuel mass is analyzed in discrete steps from zero to one hundred percent, yet this still results in thousands of unique aircraft configurations. Each of these must then be evaluated across ranges of dynamic pressure and Mach values to ensure stability at all the various flight conditions previously mentioned.

The aeroelastician typically influences the design process in three distinct phases. First, they act as stakeholders during the design stage by establishing specific structural requirements, such as defining minimum frequency thresholds for wing bending or setting stiffness targets for control surface linkages. Second, as participants in the cyclical product development process, they analytically and numerically evaluate each new product iteration and provides

feedback to the design organization. Lastly, they perform a critical verification role for the mature design, where various aircraft configurations are analyzed and, critically, tested to ensure they remain free of aeroelastic instabilities in the specified flight envelope.

A hierarchy of tools are needed to handle these phases, and the multitude of questions that need answering. On one end are low-fidelity linear models, essential for scanning thousands of scenarios to ensure flutter-free flight envelopes. On the other are high-fidelity non-linear simulations used to probe specific, critical conditions and detail studies. An efficient profit-driven organization desires to find the "optimum fidelity", models that are "good enough" to ensure safety and performance without the prohibitive cost of over-engineering or endless simulation and testing.

To perform the necessary numerical calculations, structural data is required for every combination of external stores and mass configuration. This information is typically sourced from the global finite element model of the aircraft. While this model is largely shared with the structural strength department, specific modifications needs to applied to adapt the model for the specialized needs of structural dynamics and flutter analysis.

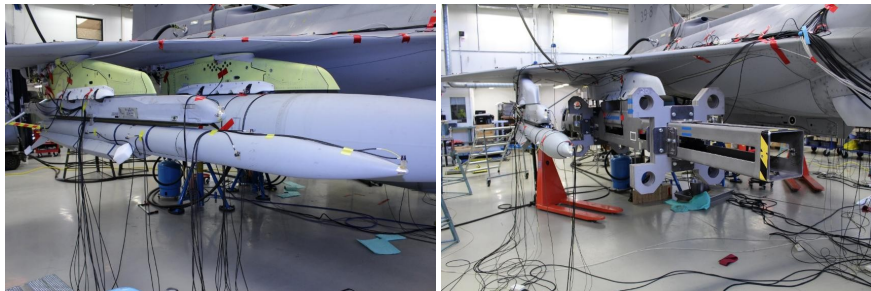
Data regarding the mass and stiffness of an aircraft configuration, derived from the finite element model, is combined with linear unsteady aerodynamics for a specific flight condition to calculate the critical flutter condition. This represents the point at which the inherent elastic and inertial forces of the structure are overcome by the forces from the airflow, causing the effective damping of the aeroelastic system to drop to zero or negative, leading to unstable vibrations that exponentially increase in amplitude.

Ground vibration tests are used to evaluate the aircraft's dynamic properties experimentally by simulating flight conditions on soft springs, exciting the structure with a known input force and measuring the response of the structure. They are conducted partly to verify, calibrate and update the finite element model, ensuring that it accurately represents the physical aircraft. However, the mass and stiffness data obtained directly from these tests can also be combined with aerodynamic data to bypass the need for a numerical structural model entirely. This approach is particularly useful during prototype development, when modifying existing aircraft, or in cases where there is limited confidence in the finite element model. Additionally, these tests provide vital information regarding structural damping, a characteristic that is not naturally included in the formulation of a linear finite element model.

While ground vibration testing is essential for both model updating and direct flutter prediction, it is also a mandatory requirement under both civilian and military regulations [4], [5]. Despite its importance, the process is exceptionally time-consuming and expensive. It also typically takes place at the very end of the product development cycle, once mature hardware is available, creating immense pressure to finish quickly so the aircraft can proceed to its first flight. Follow-up tests are usually performed later to adapt the structural model to design updates or to integrate new external stores, but these are similarly

constrained by tight schedules and a high demand for available test aircraft.

Due to these constraints, only the most representative or technically challenging aircraft configurations are selected for ground vibration testing. Examples include a clean aircraft without any external stores, configurations at maximum weight capacity, or one with external stores that have been shown to be challenging in previous stages of the product development process. Large and heavy loads often include external fuel tanks, which are used to provide the extra fuel necessary to extend the operational range of the aircraft.



(a) Elastic store and drop tanks.

(b) Elastic store and dummy drop tanks.

**Figure 1.0.2:** Ground Vibration Tests have been performed with both fuel-filled drop tanks, and solid equivalent dummies. The tests were done at differing times, and on different aircraft individuals.

External fuel tanks are, for all the reasons just mentioned, often included in several configurations of interest for ground vibration testing of the JAS 39 Gripen E, and most probably with other similar aircraft. Involving fuel tanks means managing fuel during testing, and that is a complex and cumbersome process. To maintain the airworthiness of the aircraft, the tanks must be filled according to correct procedure, through an aircraft, at a fueling station on the flight line. The tanks then have to be dismounted, moved and mounted to the test aircraft. Finally, the fuel must be disposed of once the testing is completed.

Beyond logistical issues, problems can arise with fuel shifting within the tanks. This movement causes the center of gravity of the aircraft to change slightly during an ongoing test campaign. It is also difficult to fill the tanks with high precision, which can lead to mass differences between the port- and starboard-mounted fuel tanks, and cause unintended asymmetrical responses.

In response to these challenges, solid dummy stores can be used, see Figure 1.0.2. These can be designed so that both the total mass, center of gravity and moment of inertia can be modified by adding or removing a series of adjustable weights. Dummy stores mimic the mass and balance of real external fuel tanks while being easy to handle and possible to model with high precision using detailed finite element simulations. For a structural dynamicist, this represents an ideal scenario!

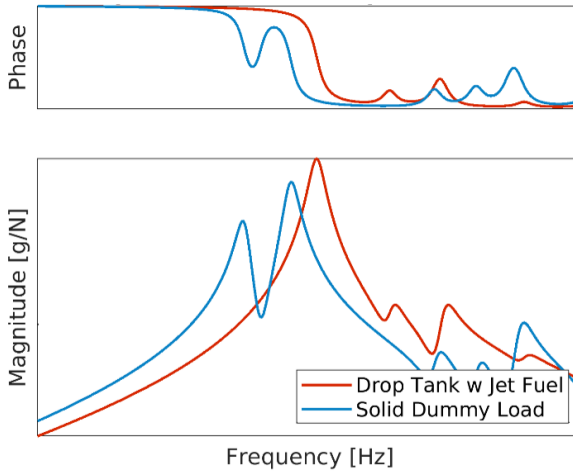


**Figure 1.0.3:** Comparison of the vertical response at a driving point, between a liquid filled drop tank and a dummy drop tank with similar mass properties.

However, when testing with dummy stores representing fuel tanks, the question arises of how well the results correspond with data from tests using actual fuel tanks. A direct comparison shows significant differences in the dynamic response, as can be observed in Figure 1.0.3. The response in the vertical direction at the forward measurement points for each test, shows that, aside from minor discrepancies, a significant natural mode is entirely absent in the case involving the liquid-filled tank.

This raises compelling questions about how the liquid content influences the dynamic response of the aircraft, which serves as a primary inspiration for this licentiate thesis.

## 1.1 Motivation

The research student in an industrial environment must navigate a tension between industrial applicability and academic depth. The employer is supporting research training with a desire of both gaining a knowledgeable employee that can handle advanced technical work, but also to gain knowledge that can be integrated into the organization and its processes. A research organization with public or government funding might prioritize long-term basic research, that can provide deep and wide impact over decades. For such an effort high-fidelity tools can always be an option, as understanding and precision are of the highest priority. The university and the supervisor desires interesting and focused research that culminates in, at least, a some expansion of the total sum of human knowledge.

This thesis exists at the boundary of "enough", investigating a specific phys-

ical phenomenon, fluid sloshing, where traditional linear models may no longer suffice. The problem is well illustrated by the observed discrepancies between ground vibration tests using fuel-filled tanks, and those using solid dummy stores, where structural behaviors present in one is absent in the other. A deeper understanding of how such nonlinear phenomena interact with the surrounding airframe allows engineers to set target requirements more precisely rather than using additional safety margins to bypass the problem.

The primary motivation for this research is to gain knowledge and understanding of local nonlinearities caused by fuel sloshing. Experimentally investigating local nonlinearities provides information on the impact on the airframe, and, in the end, supports the development and implementation of more efficient computational methods. Better understanding of these phenomena, and better tools, can significantly reduce the cost of product development by minimizing the amount of late-stage design changes that are needed to ensure safety.

## 1.2 Research aim and research questions

The primary goal of this research is to explore how specific local nonlinear phenomena, including fuel sloshing and structural variations, influence the aeroelastic performance and stability of an aircraft. To address this goal, the following research questions have been formulated:

- RQ 1:** To what extent do manufacturing variations in composite wings contribute to the discrepancies observed between predicted behavior and experimental results?
- RQ 2:** What are the specific hydroelastic effects of fuel sloshing on the dynamic behavior, structural damping, and the overall flutter envelope of a typical fighter jet?
- RQ 3:** How effectively can complex fluid-structure interactions be captured using a six-degree-of-freedom robotic excitation system, and what are the primary advantages of this approach compared to traditional ground vibration testing setups?

To answer these questions, this thesis employs proven and novel experimental techniques to isolate these nonlinear effects and quantify their impact on the aircraft's dynamic stability. The data and information should act as a solid foundation for the development of mid-fidelity simulation models.

## 1.3 Scope

The high computational cost of detailed simulations often prevents the use of high-fidelity models in a standard production environment, limiting their use to specific cases and detailed studies. At the same time, the use of fast, linear models can miss, or underestimate, the impact of non-linear phenomena.

## CHAPTER 1. INTRODUCTION

This project aims to aid in the development of efficient, lower-cost mid-fidelity methods that are practical for scenarios where thousands of individual analyses must be performed.

It is assumed that aerodynamic forces remain invariant across all analyzed scenarios. Consequently, the aerodynamic component is considered out of scope. The focus of this research is directed exclusively toward the structural aspects of the aeroelastic challenge.

The following chapters provide the theoretical background for these phenomena, a description of the experimental methodologies employed, and an analysis of the results that address the research questions.

## 2 Background

### 2.1 Aeroelasticity

Aeroelasticity is the science that deals with fluid-structure interaction; or the interaction of aerodynamic, elastic and inertial forces; or simply the static and dynamic responses of an elastic aircraft. The field is closely related to both structural dynamics and flight mechanics, as described in the classic illustration in Figure 2.1.1 by Collar [6].

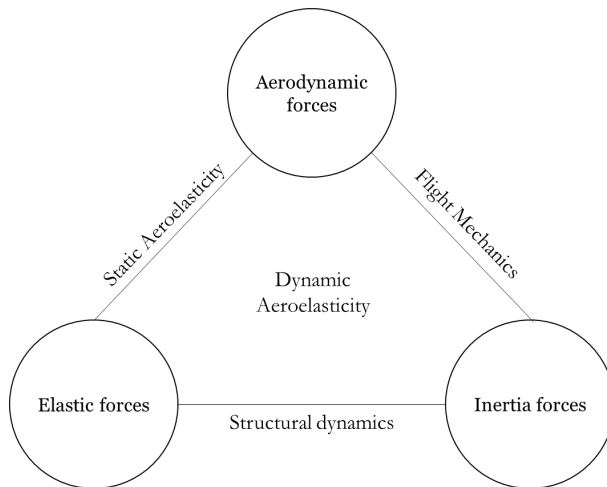


Figure 2.1.1: The aeroelastic triangle, adapted from Collar [6].

An aircraft wing subject to external loading will deform even if it is capable of sustaining the load. A deformed structure experiences a different set of aerodynamic loads compared to the undeformed structure. As aerodynamic loads increase with the speed there will be a critical speed where the static aerodynamic load that the deformed structure is subject to, grow larger than the elastic restoring forces and the deformation increases until the structure fails. This static instability is known as divergence.

Flutter, which is a subset of dynamic aeroelasticity, is a phenomenon where a transversely oscillating wing in uniform, undisturbed flow periodically gains energy from the air stream. If the energy gained is greater than the elastic and inertial resistance, the amplitude of the motion will increase and the wing is said to be fluttering.

## 2.2 Sloshing

Sloshing is intuitively known by everyone who has carried an open mug of coffee from one room to another, as it is the tendency of the free surface to undergo large motion due to relatively small movements of the container. It is defined as the movement of a liquid with a free surface inside a container, and it can be incited both by harmonic motion and transient motion [7]. The wave motion of an inviscid incompressible fluid in a rigid tank can be modeled by the free-boundary potential flow equations, presented for example by Abramson [8], [9]. A liquid inside a container has an infinite number of natural frequencies, but generally only the lowest few modes can be excited by the motion of an aircraft, and are therefore of interest in sloshing dynamics [10]. When considering full containers without a free surface, they are not subject to sloshing dynamics and are often equated to solid-mass objects.

The influence of liquid fuel movement in aircraft have been a subject of interest for the aircraft design community for many years. Test pilots have observed how sloshing in partially filled fuel tanks impact aircraft stability and control since the introduction of aviation [11].

Historically, the absence of appropriate methodologies and instruments has resulted in the industry's neglect of addressing these effects through theoretical approaches. Instead, the issue has been predominantly tackled through empirical means, by keeping the tanks as full or as empty as possible to minimize the free surface [8]. Failing that, baffles, sections, foam inserts and other measures have been used to minimize the free surface, and the amplitude of the moving liquid. For most air planes, fuel has been modeled as concentrated masses, or when the stiffness contribution of the fuel has to be considered, a simple equivalent mass oscillator coupled with the structure of interest [8], [12]–[14].

At Saab, there are three main areas of interest regarding the effects of liquid sloshing.

- Dynamic loads related to fluid within tank internal systems and structures are prominent concerns. For instance, fuel tanks may house components such as pipes and electrical cables. These elements must be engineered to endure the stresses and forces caused by the liquid. Such forces arise from various scenarios, including the dynamic response of manouvers in flight, unexpected gusts, impact during landing, as well as impacts from bird strikes. Proper sizing and material selection are essential to ensure the integrity and reliability of these internal components

under such conditions.

- The implications of fluid dynamics on the stability and control mechanics of aircraft. This consideration becomes crucial when evaluating fighter jets, which undergo a broader spectrum of maneuvers compared to commercial passenger planes.
- The effect on the flutter envelope of high-performance fighter jets. The liquid-filled internal and external fuel tanks has an added-mass effect on the aeroelastic system as a whole, but there is also a hydro-elastic effect from the sloshing that is traditionally not included in computational flutter prediction. The impact, or lack thereof, on the aeroelastic, and aeroservo-elastic, system is important to estimate for flutter practitioners to save on both simulation as well as experimental evaluation efforts.

The phenomenon of sloshing within aircraft has not received significant attention in the context of flight flutter analysis and experimental evaluation. This can be attributed in part to the strategies aimed at mitigating the issue through design modifications, and the financial burden and the increased complexity associated with addressing sloshing effects analytically or numerically for all relevant flight conditions. Demonstrating aeroelastic stability for an aircraft that is intended to carry a number of different external stores requires making use of both analysis and testing. Adding fuel fill levels as a parameter will drastically increase the number of configurations that need to be analyzed, making testing an unsuitable tool to determine the stability margins [15].

Recently, there has been a renewed focus on numerical predictions of the effect of internal fuel sloshing on aircraft structures, but there is still a lack of maturity in models and tools that make practitioners to often still exclude the hydro-elastic effect of sloshing [16], [17].

### 2.2.1 Types of motion

A liquid in a container has an infinite amount of natural frequencies, but in general it is the lower modes that will be excited by the motion of an aircraft. The liquid can move in many and fascinating ways, including planar, non-planar, rotational, beating, symmetric and chaotic motion [10]. There are a number of non-linear effects that can affect liquids in moving containers resulting in a strong dependence on amplitude.

An external fuel tank filled with liquid is subject to three different main domains of dynamic motion:

- Lateral motion induces the formation of standing waves within the tank, which can interact with the dynamic structural response of the tank. It should be noted that even a relatively low amplitude of excitation is suf-

ficient to produce such standing waves. This phenomenon has been documented in studies by Firouz & Abadi, and Pizzoli *et al* [18], [19].

- Rolling motion - generates planar and rotational motion at low amplitude excitation [19].
- Vertical motion - In contrast to lateral and rolling motions, low amplitude vertical motion typically results in the fluid surface remaining mostly flat. Any perturbations are minor and usually take the form of 'fluid fingers', a beating motion in response to the frequency of the external excitation [8].

A high amplitude of motion of any type may cause the liquid to behave chaotically [7].

### 2.2.2 Scaling a model for fluid-structure interaction experiments

Building models of one's work to aid understanding has been an important task for engineers for centuries. When performing an experimental evaluation, it is often essential for the scale model to accurately represent a certain quantity of the larger object. In such cases, there are a number of strategies that can be employed depending on what quantity is important.

For hydrodynamics there are three different kinds of similarities that may need to be maintained: geometric similarity, kinematic similarity and dynamic similarity. If the kinematics and dynamic behavior of the liquid in a reduced-sized closed container are supposed to mimic that of the liquid in a larger container, then a strategy is to maintain Reynolds-Froude scaling, i.e. constancy of the Reynolds and Froude numbers [20]. While several other dimensionless quantities, such as the Cauchy number, the cavitation number and the Weber number also can be considered, the Froude and Reynolds numbers are the most impactful signifier of scale adherence [7].

Reynolds number is defined as a dimensionless quantity that states the ratio of inertial forces to viscous forces [21]. It is a characterization of the fluid as it interacts with an object or a boundary

$$Re = \frac{uL}{\nu} = \frac{\rho uL}{\mu}, \quad (2.2.1)$$

where  $u$  is the flow velocity,  $L$  is the characteristic length,  $\nu$  is the kinematic viscosity,  $\mu$  is the dynamic viscosity of the fluid, and  $\rho$  is the density of the fluid. Notably, it varies linearly with both  $u$  and  $L$ .

The Froude number, another dimensionless quantity, is derived from the ratio of velocity to characteristic length

$$Fr = \frac{u}{\sqrt{gL}}. \quad (2.2.2)$$

This number illustrates the correlation between the inertia of flow or its viscosity and the prevailing local force field, which is often gravitational,  $g$ , in nature.

Since sloshing is associated with gravity waves, this is a critical factor to maintain [7]. Maintaining Froude scaling involves preserving this ratio that linear in relation to the flow velocity  $u$ , but proportional to the square root of the characteristic length  $L$ .

For fuel sloshing in an aerospace context we are mainly concerned with the scaling between a jet fuel such as JP-8 (the main standard for military use) and the experimental liquid, in this case water. Comparing the density and viscosity of JP-8 and water, from the data in Table 2.2.1, one can see that the ratio  $\rho/\mu$  for water at room temperature is 2-2.5 times higher than for JP-8.

	JP-8	Tap water
Density [kg/L]	0.775-0.840 [22]	0.997
Viscosity, at 20C [mm <sup>2</sup> /s]	1.65 - 1.95 [23]	1.0
Viscosity, at -20C [mm <sup>2</sup> /s]	4.52 [24]	-

**Table 2.2.1:** Fluid properties for JP-8 and tap water.

Geometric, mechanical and kinematic scaling can be used to further alter the Froude and Reynolds numbers of the scale model to match that of the full-scale version. For other purposes, an emphasis on accurate geometrical scaling, mechanical scaling, strain scaling, or frequency scaling might be more suitable [7]. All of these strategies aim to preserve the constancy of some quantity [20].

### 2.2.3 Numerical sloshing analysis

The natural frequencies and associated fuel movement depend greatly on the shape of the container. Early developments in the numerical treatment of the natural frequencies and associated fuel motions for rigid containers with rectangular and cylindrical (standing) cross sections were made by Rayleigh, Stekloff and Lamb [25]–[27]. Budiansky and Chu [28], [29] made significant contributions for horizontal cylindrical containers and arbitrary fill levels. Budiansky built on Lamb’s work to determine the free-surface liquid natural frequencies and mode shapes for the horizontal cylindrical container, which was more difficult because of the non-straight walls of the container [28]. Chu created a numerical method to determine the kernel function part of the Neumann function in the Budiansky solution, which allowed the analysis of arbitrary levels of liquid fill [29].

Modern solutions to the sloshing problem employ different types of Computational Fluid Dynamics (CFD) methods to model fluid flow, including violent sloshing flow. There are many methods, but they can generally be divided into *potential flow methods* and *Navier-Stokes methods* [7]. The Smoothed Particle Hydrodynamics (SPH) method, and the Volume of Fluid (VOF) method, both different types of Navier-Stokes methods, have recently been evaluated by the SLOWD project, a EU-financed project aiming to investigate the use of fuel

slosh to reduce the design loads on commercial aircraft structures [17], [30], [31].

Recently, other analytical methods have begun to be used in numerical sloshing analysis, such as machine learning methods, black-box models, and equivalent mechanical models - as well as a combination of these [32]. A thorough exploration of numerical analysis will not be undertaken at this time, instead it will be elaborated on in detail only when it proves essential for the project.

### 2.2.4 Experimental sloshing investigations

Early experimental testing of the effect of pitching oscillations of a wing-mounted external fuel tank was carried out by Widmeyer and Reese at NACA Langley in 1953 [33]. They found two different damping regimes, where an empty and full tank behaved similarly (when accounting for the added mass effect) and that fill levels between 20-80% also had a similar damping regime.

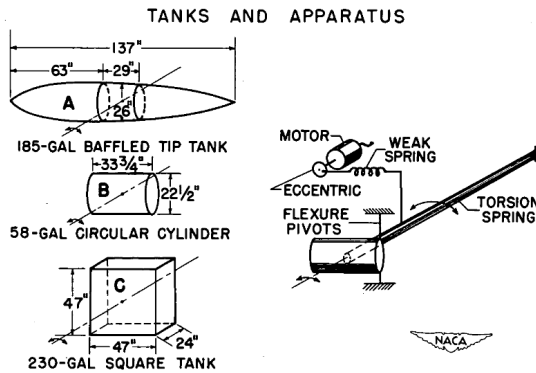


Figure 2.2.2: The pitch oscillation apparatus used by Widmeyer and Reese [33].

Ikeda and Nakagawa [34] investigated the vertical sinusoidal excitation of an elastic system of a cantilevered beam with rectangular acrylic tank filled with liquid, specifically with a natural frequency about twice that of the liquid. They found that as the excitation frequency approached the natural frequency of the system, the liquid surface was excited, and energy was transferred from the structure to the free surface. They also found that structural damping was related to the fill level of the tank, with a higher degree of damping for higher fill levels.

Martinez-Carrascal and González-Gutiérrez [35] performed a Froude scaled experiment with a single degree-of-freedom spring-damper system, and could confirm that the presence of fluid increased the damping notably and that the damping consists of both an inertial term and a dissipative term.

Saltari [36] employed an electrodynamic shaker to generate vertical vibrational input for wing tanks through a sine sweep, which induced chaotic liquid motion within the tank, and intense impacts between the liquid and the tank's walls. This chaotic interaction facilitates energy dissipation, offering a potential damping effect for the structure connected to the tank.

Constantin *et al.* [37] built on the work by Saltari and performed a scaled experiment of a wing tank with a 50% fill level to validate the findings of a substantial dissipative damping component. An effect could be demonstrated regardless of the excitation amplitude. A model of the dry structure coupled with a 1DOF surrogate model interpolated from the experimental data collected by Martínez-Carrascal and González-Gutiérrez was shown to predict the induced damping.

Debshütz *et al.* [38] at Airbus and DLR performed an experimental investigation of a generic fighter jet wing tank, in order to gather reliable data to tune analytical reduced-order models. They used a fuel container in a representative shape of a wing tank in a fighter jet and mounted it to an industrial robot to simulate flight maneuvers. By careful consideration the experiment was kept as similar as possible to real conditions, with both Froude and Reynolds numbers in the same order of magnitude in both the planned scenario and final model.

### 2.3 Sloshing and aeroelasticity

Farhat *et al.* [16] compares a frozen mass model and a hydro-elastic model of a wing-store configuration with varying fill levels and find that ignoring the hydro-elastic effect leads to an underestimation of the critical pressure and flutter speed. A multi-physics simulation of a pitch-plunge aerofoil with an externally carried fuel mass shows that the hydro-elastic effect, ignoring the added-mass effect, is to raise the flutter boundary at transonic speeds but that effect is lower at lower Mach numbers [39].

Pizzoli [19] uses a reduced-order model based on an equivalent mechanical mass method to investigate the effect of an under-body-mounted fuel tank on the body-freedom flutter research model. A partially filled rigid fuel tank was integrated into an existing aeroservo-elastic model of the aircraft and compared to a frozen mass model integrated in the same way. He finds an effect on the lateral dynamics of the aircraft, with the dutch roll mode coupling with the sloshing behavior and becoming unstable.



# 3 Materials and methods

## 3.1 Structural dynamics

The equations of motion for multi degrees-of-freedom (MDOF) systems with general viscous damping can be written as

$$M\ddot{\mathbf{x}}(t) + C\dot{\mathbf{x}}(t) + \mathbf{K}\mathbf{x}(t) = \mathbf{F}(t), \quad (3.1.1)$$

where  $M$  is the mass matrix,  $C$  is the damping matrix,  $\mathbf{K}$  is the stiffness matrix,  $\mathbf{x}$  is deformation vector, and a dot denotes differentiation with respect to time. Finally,  $\mathbf{F}$  is a force vector acting on the system.

Modal parameters are derived by assuming free vibrations and negligible damping. If there is no damping and no applied loads in the system, the equations of motion reduces to

$$M\ddot{\mathbf{x}} + \mathbf{K}\mathbf{x} = \mathbf{0}, \quad (3.1.2)$$

where the explicit indication of time dependency has been dropped for convenience. Following Inman [40], we can assume that the solution has the form

$$\mathbf{x}(t) = \mathbf{v}e^{j\omega t}, \quad (3.1.3)$$

where  $\mathbf{v}$  is a nonzero vector,  $\omega$  is a constant, and  $j = \sqrt{-1}$ . It is noted that  $e^{j\omega t} = \cos \omega t + j \sin \omega t$  by the Euler formula. Differentiating (3.1.3) twice yields the acceleration vector

$$\ddot{\mathbf{x}}(t) = -\omega^2 \mathbf{v}e^{j\omega t}. \quad (3.1.4)$$

Substituting (3.1.4) into (3.1.2) gives

$$(-\omega^2 \mathbf{M} + \mathbf{K})\mathbf{v}e^{j\omega t} = \mathbf{0}. \quad (3.1.5)$$

Since (3.1.5) must hold for all  $t$ , the non-trivial solution for  $\omega$  and  $\mathbf{v}$  must satisfy

$$(-\omega^2 \mathbf{M} + \mathbf{K})\mathbf{v} = \mathbf{0}. \quad (3.1.6)$$

(3.1.6) can be reformulated as an eigenvalue problem. The standard eigenvalue problem can be written as

$$\mathbf{A}\mathbf{v} = \lambda\mathbf{v} \Leftrightarrow (\mathbf{A} - \lambda\mathbf{I})\mathbf{v} = \mathbf{0}.$$

Assuming that  $M$  is a positive semidefinite matrix and has an inverse, our problem can be rewritten on the standard form by multiplying both sides of (3.1.6) with  $M^{-1}$ , taking  $\mathbf{A} = M^{-1}\mathbf{K}$ . It becomes

$$(M^{-1}\mathbf{K} - \omega^2\mathbf{I})\mathbf{v} = \mathbf{0}, \quad (3.1.7)$$

where  $\lambda = \omega^2$  is identified as the eigenvalue. The solution is given by a list of eigenvalues  $\lambda_i$  with related eigenvectors  $\mathbf{v}_i$ . This is indicated by re-writing (3.1) as

$$(M^{-1}\mathbf{K} - \lambda_i\mathbf{I})\mathbf{v}_i = \mathbf{0}, \quad i = 1, 2, \dots, n. \quad (3.1.8)$$

Each pair of eigenvalue and eigenvector gives a solution to (3.1.2) of the form (3.1.3), called an eigenmode. The general solution is a linear combination of all eigenmodes.

The eigenvectors can also be called the *mode shape* vectors. The mode shapes can be thought of as displacement patterns which describe how the system moves at each cyclic natural frequency  $\omega_i$  [41].

The eigenvalues  $\lambda_i = \omega_i^2$  can be collected in a diagonal eigenvalue matrix as follows

$$\underset{(n \times n)}{\boldsymbol{\lambda}} = \begin{bmatrix} \lambda_1 & 0 & 0 & 0 \\ 0 & \lambda_2 & 0 & 0 \\ 0 & 0 & \ddots & 0 \\ 0 & 0 & 0 & \lambda_n \end{bmatrix}.$$

The eigenvectors can be collected in a mode shape matrix as follows

$$\underset{(n \times n)}{\mathbf{V}} = \left[ \begin{array}{c} \left\{ \begin{array}{c} v_{11} \\ v_{21} \\ \vdots \\ v_{n1} \end{array} \right\} \left\{ \begin{array}{c} v_{12} \\ v_{22} \\ \vdots \\ v_{n2} \end{array} \right\} \dots \left\{ \begin{array}{c} v_{1n} \\ v_{2n} \\ \vdots \\ v_{nn} \end{array} \right\} \end{array} \right].$$

where each column vector in the modal matrix corresponds to a specific mode shape. These vectors can be arbitrarily scaled as they only show relative motions between degrees of freedom at each eigenvalue, [3].

The mode shapes are orthogonal when weighted with either the mass matrix  $M$  or the stiffness matrix  $\mathbf{K}$ . Multiplying these system matrices with  $\mathbf{V}$  on both sides yields the diagonal matrices

$$\mathbf{V}^T\mathbf{M}\mathbf{V} = \begin{bmatrix} m_1 & 0 & 0 & 0 \\ 0 & m_2 & 0 & 0 \\ 0 & 0 & \ddots & 0 \\ 0 & 0 & 0 & m_n \end{bmatrix}, \quad (3.1.9)$$

and

$$\mathbf{V}^T \mathbf{K} \mathbf{V} = \begin{bmatrix} k_1 & 0 & 0 & 0 \\ 0 & k_2 & 0 & 0 \\ 0 & 0 & \ddots & 0 \\ 0 & 0 & 0 & k_n \end{bmatrix}, \quad (3.1.10)$$

where  $m_i$  is the generalized mass and  $k_i$  is the generalized stiffness for mode  $i$ . Since these values depend on an arbitrary modal scaling the values may not have any real physical meaning. However, the ratio between the generalized mass and the generalized stiffness is fixed since it is related to the undamped natural frequencies as

$$\omega_i = \sqrt{k_i/m_i}. \quad (3.1.11)$$

Typically, each mode shape is associated with a natural frequency  $\omega_i$  and the generalized mass  $m_i$ .

Importantly, if a structure is not constrained in space it is possible for the structure to move as a rigid body. For each degree-of-freedom where rigid body motion is possible there exists one natural frequency that is zero. These are called rigid body modes, and exist when free-free boundary conditions are used.

### 3.1.1 Experimental modal analysis

Experimental modal analysis aims to identify the dynamic properties of a structure through testing, see Figure 3.1.1 for an example of a Ground Vibration Test (GVT) of a Gripen E aircraft.



Figure 3.1.1: Ongoing ground vibration test of a JAS 39 Gripen E aircraft.

This is done by measuring a dynamic input force and the resulting displacement, velocity or acceleration, principally illustrated in Figure 3.1.2. Most commonly acceleration is measured [40], [41].

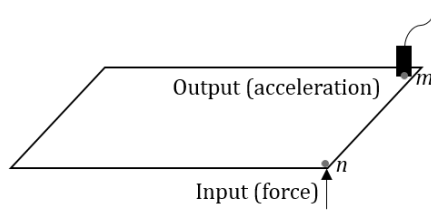


Figure 3.1.2: Example of force and response on a simple plate.

A typical setup for experimental modal analysis using shaker excitation is shown in Figure 3.1.3. An analyzer / test data manager sends an excitation signal through an amplifier to an electrodynamic shaker. The shaker is connected to the test object through a weak stinger rod, ensuring that only the force component perpendicular to the surface is transferred. Between the stinger rod and the test object is a force transducer, measuring the resulting input force. The test object is equipped with a number of accelerometers, the output of which is connected back to the analyzer / test data manager, that collates and analyzes the test data. An overview of the analysis process is shown in Figure 3.1.4.

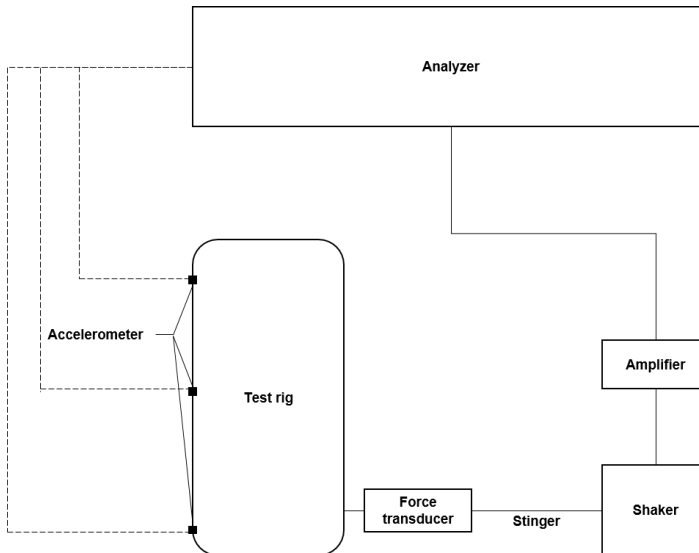


Figure 3.1.3: Overview of a generic test setup employing shaker excitation.

The time domain accelerations are converted to the frequency domain for further analysis, via a Fourier transform. Frequency response functions (FRFs) are then calculated, as a representation of the output response in a specific point to an applied force in a specific point. The FRFs are complex-valued func-

tions whose phase and magnitude components represent the ratio of output response to a given input force.

When measuring accelerations in the time domain, the equivalent output in the frequency domain will be an *accelerance* FRF. For the system in (3.1.1) the general frequency response function can be written as

$$H_{mn}(\omega) = -\omega^2 \sum_{r=1}^N \frac{v_{mr}v_{nr}}{m_r} \frac{1}{j2\omega\xi_r\omega_r - \omega^2 + \omega_r^2}, \quad (3.1.12)$$

which describes the response as the sum over  $N$  nodes, with acceleration at DOF  $m$ , for a force at DOF  $n$ . It can be seen that this expression contains the mode shapes, their related natural frequencies and viscous modal damping ratios.

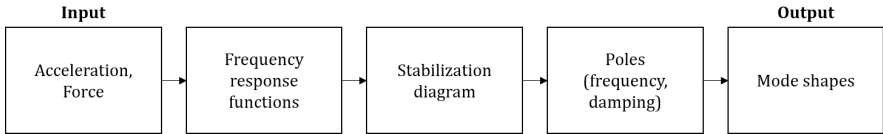


Figure 3.1.4: Analysis process in experimental modal analysis.

The FRF that measures the output response in the input point ( $H_{nn}$ ) is called a *driving point measurement*, and it has some specific characteristics: all resonances are separated by anti-resonances with a minimal magnitude, and the FRF loses  $180^\circ$  of phase over a resonance and gains  $180^\circ$  over an anti-resonance. These characteristics are useful quality checks during experimental testing, as irregular driving point FRFs can be caused by faulty or improperly aligned equipment [42].

The denominator of (3.1.12) are the poles, and they contain information about damping and natural frequencies of the eigenmodes [40]. Displaying the poles for an increasing number of modes in the model (model order) on the frequency axis helps sort the true modes from ones stemming from noise (e.g. measurement noise, and numerical noise) as the estimation of frequency and damping for a true mode should be stable no matter the model order of the curve fitting [42], [43]. Choosing the model order high enough is necessary in order to find all the physical modes, due to the presence of noise in the data.

### 3.2 Aeroelasticity

Following Borglund & Eller [44], the aeroelastic equation of motion for a MDOF system can be written on the same form as (3.1.2), with an applied external load,

$$M\ddot{\mathbf{x}} + \mathbf{K}\mathbf{x} = \mathbf{f}_{tot}(t). \quad (3.2.13)$$

This gives that at the steady state where  $\ddot{\mathbf{x}} = 0$  there is an equilibrium between the elastic forces and the total external forces

$$\mathbf{K}\mathbf{x} = \mathbf{f}_{tot}. \quad (3.2.14)$$

There are several components that make up the total external forces: Aerodynamic forces  $\mathbf{f}_a$  due to elastic deformation  $\mathbf{x}$  and control surface deflection  $\delta$ , aerodynamic forces due to small changes of the reference geometry  $\mathbf{f}_{a0}$ , and the constant load from for example changes in mass distribution  $\mathbf{f}_w$ .

The aerodynamic forces can be formulated as

$$\mathbf{f}_a = q\mathbf{Q}_0\mathbf{x} + q\mathbf{f}_0\delta, \quad (3.2.15)$$

where  $\mathbf{Q}_0$  is the steady state aerodynamic matrix,  $\mathbf{f}_0$  is the steady state force vector and  $q$  is the dynamic pressure. Assuming that small changes in the reference geometry can be expressed by an elastic deflection vector  $\mathbf{x}_0$  then

$$\mathbf{f}_{a0} = q\mathbf{Q}_0\mathbf{x}_0, \quad (3.2.16)$$

so the total external force  $\mathbf{f}_{tot}$  becomes

$$\mathbf{f}_{tot} = \mathbf{f}_a + \mathbf{f}_{a0} + \mathbf{f}_w = q\mathbf{Q}_0\mathbf{x} + q\mathbf{f}_0\delta + q\mathbf{Q}_0\mathbf{x}_0 + \mathbf{f}_w,$$

and (3.2.14) can be written as

$$\mathbf{K}\mathbf{x} = q\mathbf{Q}_0\mathbf{x} + q\mathbf{Q}_0\mathbf{x}_0 + q\mathbf{f}_0\delta + \mathbf{f}_w. \quad (3.2.17)$$

If  $\mathbf{x}$  represents the change in elastic deflection with respect to the undeformed state  $\mathbf{x}_0$  then the total change in geometry is  $\mathbf{x}_0 + \mathbf{x}$  which means that (3.2.17) can be re-written as a linear systems of equations, given by

$$[\mathbf{K} - q\mathbf{Q}_0]\mathbf{x} = \mathbf{f}_{a0} + \mathbf{f}_{a\delta} + \mathbf{f}_w = \mathbf{f}_{tot}. \quad (3.2.18)$$

#### 3.2.1 Flutter

It is convenient to tackle flutter in the frequency domain as that provides a complete description of possible motion for a linear stability problem [45]. Starting with the general aeroelastic equation of motion from (3.2.13) we can disregard the external forces that does not depend on the elastic deformation as they will not influence stability in the eventual linear approximation [44]. This gives

$$M\ddot{x} + Kx = f_a(t) = qQ_0x, \quad (3.2.19)$$

with the the steady-state aerodynamic matrix  $Q_0$  or  $Q(0)$ . This can be re-formulated, analogous with (3.1.3) - (3.1.6) in the previous section, as the frequency-domain equations of motion

$$Mp^2v + Kv = qQ(\hat{p})v, \quad (3.2.20)$$

where the aerodynamic transfer matrix  $Q(\hat{p})$  depends on the reduced Laplace variable  $\hat{p} = pb/u$ .  $b$  is the aerodynamic reference length, often the wing semi-chord, and  $u$  the airstream velocity.

By re-arranging (3.2.20) we get the *nonlinear* eigenvalue-problem

$$F(p)v = [Mp^2 + K - qQ(\hat{p})]v = 0, \quad (3.2.21)$$

where  $p$  is the eigenvalue resulting in a singular flutter matrix  $F(p)$  and  $v$  is the eigenvector. Assuming that the problem can be solved for a set of eigenvalues  $p_j$ , with eigenvectors  $u_j$  at any dynamic pressure  $q$ , the eigenvectors represent the mode shapes and the eigenvalues contain damping  $\sigma_j = \text{Re } p_j$ , and frequency  $\omega_j = \text{Im } p_j$ . At  $q = 0$  we find the vibration problem from (3.1.6) again

$$[p^2M + K]v = 0, \quad (3.2.22)$$

with known solutions  $p_j = i\omega_j$  ( $p_j^2 = -\omega_j^2$  at positive frequencies).

Most aerodynamic methods used for stability analysis provides the frequency-domain forces  $Q(ik)$  or  $Q(k)$  rather than the transfer matrix  $Q(\hat{p})$  for arbitrary motion. However, since the structure will experience undamped vibrations at the flutter boundary,  $Q(k)$  will be correct at that point.  $Q(k)$  is possibly a an approximation of  $Q(\hat{p})$  for weakly damped motion when  $\hat{p}$  is close to the imaginary axis.

This means that a solution  $p = ik$  to the approximate *linear* eigenvalue problem

$$\left[ \left(\frac{u}{b}\right)^2 Mp^2 + K - qQ(k) \right] v = 0, \quad (3.2.23)$$

is also a solution the full nonlinear eigenvalue problem (3.2.21). Given that  $Q(k)$  is available, the problem now reduces to solving (3.2.23) for a given air-speed.

### 3.2.2 The p-k method

The basic principle of the  $p$ - $k$  method is to iteratively solve the problem by considering the reduced frequency  $k$  in  $Q(k)$  as a parameter. For a given value of  $k$  we solve a linear eigenvalue problem for a set of eigenvalues  $\hat{p}_j^2(k)$  and consider the square roots  $\text{Im } \hat{p}_j(k) > 0$ .

If any of the solutions satisfies

$$\text{Im } \hat{p}_j(k) = k, \quad (3.2.24)$$

or, rather, approximates it to within a suitable tolerance, it must be an eigenvalue  $\hat{p}$  to (3.2.21).

Using direct iteration gives the algorithm

$$k^{l+1} = \text{Im } \hat{p}(k^l), \quad (3.2.25)$$

with the condition

$$\left| \text{Im } \frac{d\hat{p}}{dk}(k^*) \right| < 1, \quad (3.2.26)$$

where  $k^*$  is a solution to (3.2.24). The basic algorithm converges slowly, and several methods are known to speed it up considerably, such as applying Newton's method to the problem [46].

## 4 Results

The results of this research are divided into the identification of manufacturing induced structural variability in composite wings and the characterization of hydroelastic effects caused by fuel sloshing in external stores.

Experimental modal testing of multiple composite wing sets revealed significant deviations from the nominal design. For one specific wing set, a frequency difference was observed in the first bending mode between the left and right wings, resulting in manufacturing induced asymmetry. These asymmetries caused the physical structure to exhibit independent left and right wing torsion modes, whereas the nominal finite element model predicted combined symmetrical and anti-symmetrical modes. To address these discrepancies, an optimization based model update was performed by adjusting material properties and geometric layup angles, which significantly improved the correlation between the numerical models and experimental data. The updated models successfully captured the shift of symmetrical mode shapes into unbalanced, single wing dominated modes [1].

The investigation into internal fluid dynamics utilized a modular wing store system to compare liquid filled and rigid mass configurations. The results demonstrated that sloshing introduces non-linear hydroelastic effects and frequency shifts that are absent in traditional frozen mass models. At a 50% fill level, a specific store sway structural mode identified in the dry configuration dissipated completely in the wet configuration due to the energy absorption of the moving fluid. While the first wing bending mode showed a consistent mass match between configurations, modes involving torsional motion exhibited pronounced frequency shifts. The use of stepped sine excitation was required to manage the lag between structural motion and fluid response, ensuring a steady state periodic measurement [2].

A more experimental setup, utilizing a six degrees-of-freedom robot was investigated. This setup allowed for the precise capture of the accelerations, motions, and forces generated by the resulting sloshing behavior. The data collection was performed using a synchronized system that integrated a high-resolution motion capture array, accelerometers, and a six-component load cell to measure forces and moments. However, the experimental setup faced challenges during tests involving vertical motion. The accuracy of the motion capture system diminished at the outer boundaries of the cameras' combined

field of view, where the tracking of the reflective markers became less consistent. Furthermore, because the forces generated by the sloshing liquid were relatively small, the measurements occurred at the lower end of the load cell's calibrated range. While the system maintained high precision and a high rate of measurement, recording data at these lower magnitudes can introduce sensitivity issues regarding the absolute accuracy of the force data [3].

Numerical flutter analysis performed on the updated wing combinations showed a significant spread in stability boundaries. Using the PK-method, the nominal model predicted a flutter critical dynamic pressure of 6.7 kPa at a Mach number of 0.5. However, the variation in dynamic properties across different wing sets led to a substantial range of critical flutter speeds [1]. Configurations with liquid filled tanks generally demonstrated a higher critical flutter velocity than their rigid counterparts. This improvement is primarily attributed to the hydroelastic effects of sloshing, which increased the frequency separation between the fundamental wing bending and torsion modes, thereby delaying the onset of aeroelastic instability. These findings indicate that ignoring hydroelastic effects typically leads to an underestimation of the flutter speed [2].

## 5 Conclusions and future work

The study demonstrates that accurate structural modeling is essential for ensuring the robustness of analytical predictions, as experimental work has shown that manufactured components can differ significantly from theoretical designs. Relying on a perfectly symmetrical nominal model is insufficient for high-precision work, as variations can significantly alter stability boundaries. While the model updating process successfully improved the correlation between numerical representations and experimental data, it is concluded that using multiple test configurations as inputs would result in a more well-rounded and accurate finite element model.

Regarding fuel dynamics, the work concludes that traditional frozen-mass numerical models are inadequate because they omit the characterization of internal fluid dynamics. The presence of fluid introduces a dissipative damping effect for certain modes of the connected structure, a potential benefit that is not included in linear models. Incorporating these hydroelastic effects into early design phases can contribute to increased structural robustness and reduced conservatism.

The research establishes that robotic excitation provides a viable alternative to traditional ground vibration testing since it can achieve the high-amplitude movements necessary to reach chaotic sloshing regimes. By integrating a high-resolution motion capture system with a six-component load cell and linear accelerometers, the research successfully produced a synchronized dataset of the forces and moments generated by the fluid

Ultimately, the study suggests that the development and implementation of efficient mid-fidelity computational methods are practical and necessary for production environments. Such tools can significantly reduce the cost of product development by minimizing the need for late-stage design changes to ensure safety and performance. This research establishes an experimental foundation for transitioning away from empirical mitigation strategies toward analytical or numerical treatments of these local non-linear phenomena.

### 5.1 Future Research Directions

Future research should prioritize the evaluation and maturation of diverse numerical methods to bridge the gap between experimental observations and ma-

ture processes, used for high-volume analyses. This includes investigating approaches such as Smoothed Particle Hydrodynamics (SPH) [47] and emerging reduced-order models based equivalent mechanical mass oscillators [19], [32]. Expanding the experimental data series is also essential to capture a fuller spectrum of hydroelastic effect across the entire operational range. This should involve testing a broader spectrum of fill levels beyond the 50% and 100% cases to better map the sloshing effects identified in literature. Furthermore, introducing fluids with differing viscosities would result in a more thorough assessment of the hydroelastic mechanisms and allow for Reynolds-Froude valid scaling of the effects of the fluid-structure interactions. Using robotic excitation should enhance the ability to characterize complex internal fluid dynamics, but care is needed to ensure the accuracy of the measured data.

## Bibliography

- [1] A. Ellmo, “Ground vibration testing and model update of a transonic flutter wind tunnel model”, in *Proceedings of the 20th International Forum on Aeroelasticity and Structural Dynamics (IFASD)*, Updated version, The Hague, Netherlands, 2024.
- [2] A. Ellmo, “Design and testing of a wing-fuel tank system for fuel-slosh studies”, in *Proceedings of the 21st International Forum on Aeroelasticity and Structural Dynamics (IFASD)*, Accepted for presentation, Göttingen, Germany, 2026.
- [3] A. Ellmo and A. Linderholt, “Sloshing tests using a six degree-of-freedom robot”, 2026, Preliminary version.
- [4] D. of Defense, “MIL-A-8870C: Airplane Strength and Rigidity, Vibration, Flutter and Divergence”, Naval Air Warfare Center Aircraft Division Lakehurst, USA, MIL-STD 8870C, Mar. 1993.
- [5] European Union Aviation Safety Agency, “Cs-25: Certification specifications for large aeroplanes”, EASA, Amendment 28, 2023.
- [6] A. R. Collar, “The expanding domain of aeroelasticity”, *The Aeronautical Journal*, vol. 50, no. 428, pp. 613–636, 1946.
- [7] O. M. Faltinsen and A. N. Timokha, *Sloshing*. Cambridge University Press, 2009.
- [8] H. N. Abramson, “The Dynamic Behavior of Liquids in Moving Containers, with Applications to Space Vehicle Technology”, Jan. 1966.
- [9] F. T. Dodge and S. Antonio, *The new ”Dynamic Behavior of Liquids in Moving Containers”*. Southwest Research Institute, San Antonio, TX, 2000.
- [10] R. Ibrahim, *Liquid Sloshing Dynamics: Theory and Applications*. Cambridge University Press, 2005.
- [11] C. C. Smith Jr, “The effects of fuel sloshing on the lateral stability of a free-flying airplane model”, Tech. Rep., 1948.
- [12] E. W. Graham and A. M. Rodriguez, “The Characteristics of Fuel Motion Which Affect Airplane Dynamics”, *Journal of Applied Mechanics*, vol. 19, no. 3, pp. 381–388, Sep. 1951.

## BIBLIOGRAPHY

- [13] H. Luskin and E. Lapin, “An Analytical Approach to the Fuel Sloshing and Buffeting Problems of Aircraft”, *Journal of the Aeronautical Sciences*, vol. 19, no. 4, pp. 217–228, Apr. 1952.
- [14] F. Cazier Jr. and R. Ricketts, “Structural dynamic and aeroelastic considerations for hypersonic vehicles”, in *32nd Structures, Structural Dynamics, and Materials Conference*, Baltimore, MD, U.S.A.: American Institute of Aeronautics and Astronautics, Apr. 1991.
- [15] E. K.-Y. Chiu and C. Farhat, “Effects of Fuel Slosh on Flutter Prediction”, in *50th AIAA/ASME/ASCE/AHS/ASC Structures, Structural Dynamics, and Materials Conference*, Palm Springs, California: American Institute of Aeronautics and Astronautics, May 2009.
- [16] C. Farhat, E. K.-y. Chiu, D. Amsallem, *et al.*, “Modeling of Fuel Sloshing and its Physical Effects on Flutter”, *AIAA Journal*, vol. 51, no. 9, pp. 2252–2265, Sep. 2013.
- [17] P. Guthrie, F. Gambioli, A. Chamos, *et al.*, *Sloshing Wing Dynamics – Project Overview*, Mar. 2020.
- [18] R. D. Firouz-Abadi, P. Zarifian, and H. Haddadpour, “Effect of Fuel Sloshing in the External Tank on the Flutter of Subsonic Wings”, *Journal of Aerospace Engineering*, vol. 27, no. 5, p. 04 014 021, Sep. 2014.
- [19] M. Pizzoli, “Investigation of Sloshing Effects on Flexible Aircraft Stability and Response”, *Aerotecnica Missili & Spazio*, vol. 99, no. 4, pp. 297–308, Dec. 2020.
- [20] S. D. Zwart, “Scale Modelling in Engineering: Froude’s Case”, in *Philosophy of Technology and Engineering Sciences*, Elsevier, 2009, pp. 759–798.
- [21] J. D. Anderson and M. L. Bowden, *Introduction to flight*. McGraw-Hill Higher Education New York, NY, USA, 2005, vol. 582.
- [22] D. of Defense, *MIL-DTL-83133 - Detail Specification - Turbine Fuel, Aviation, Kerosene Type, JP-8 (NATO F-34) AND NATO F-35*, Mar. 2025.
- [23] T. J. Fortin and A. Laesecke, “Viscosity Measurements of Aviation Turbine Fuels”, *Energy & Fuels*, vol. 29, no. 9, pp. 5495–5506, Sep. 2015.
- [24] L. E. Caceres-Martinez and G. Kilaz, “Kinematic viscosity prediction of jet fuels and alternative blending components via comprehensive two-dimensional gas chromatography, partial least squares, and Yeo-Johnson transformation”, *Journal of Separation Science*, vol. 47, no. 5, p. 2 300 816, Mar. 2024.
- [25] L. Rayleigh, “XVII. *On the maintenance of vibrations by forces of double frequency, and on the propagation of waves through a medium endowed with a periodic structure*”, *The London, Edinburgh, and Dublin Philosophical Magazine and Journal of Science*, vol. 24, no. 147, pp. 145–159, Aug. 1887.
- [26] W. Stekloff, “Sur les problèmes fondamentaux de la physique mathématique”, *Annales scientifiques de l’École normale supérieure*, vol. 19, pp. 191–259, 1902.
- [27] H. Lamb, *Hydrodynamics*. Dover Publications, 1945.

- [28] B. Budiansky, "Sloshing of Liquids in Circular Canals and Spherical Tanks", *Lockheed Aircraft Corporation*, 1960.
- [29] W.-H. Chu, "Fuel sloshing in a spherical tank filled to an arbitrary depth", *AIAA Journal*, vol. 2, no. 11, pp. 1972–1979, 1964.
- [30] L. C. Malan, C. Pilloton, A. Colagrossi, *et al.*, "Numerical Calculation of Slosh Dissipation", *Applied Sciences*, vol. 12, no. 23, p. 12 390, Dec. 2022.
- [31] P. Sun, C. Pilloton, M. Antuono, *et al.*, "Inclusion of an acoustic damper term in weakly-compressible SPH models", *Journal of Computational Physics*, vol. 483, p. 112 056, Jun. 2023.
- [32] M. Pizzoli, F. Saltari, G. Coppotelli, *et al.*, "Neural-network-based reduced order modeling for nonlinear vertical sloshing with experimental validation", In Review, preprint, Jul. 2022.
- [33] E. J. Widmeyer and J. R. Reese, "Moment of inertia and damping of fluid in tanks undergoing pitching oscillations", NACA, Research Memorandum, Jun. 1953, NACA RM L53E01a.
- [34] T. Ikeda and N. Nakagawa, "Non-linear vibrations of a structure caused by water sloshing in a rectangular tank", *Journal of Sound and Vibration*, vol. 201, no. 1, pp. 23–41, 1997.
- [35] J. Martinez-Carrascal and L. González-Gutiérrez, "Experimental study of the liquid damping effects on a SDOF vertical sloshing tank", *Journal of Fluids and Structures*, vol. 100, p. 103 172, Jan. 2021.
- [36] F. Saltari, M. Pizzoli, G. Coppotelli, *et al.*, "Experimental characterisation of sloshing tank dissipative behaviour in vertical harmonic excitation", *Journal of Fluids and Structures*, vol. 109, p. 103 478, Feb. 2022.
- [37] L. Constantin, J. J. De Courcy, B. Titurus, *et al.*, "Effect of fuel sloshing on the damping of a scaled wing model - experimental testing and numerical simulations", *Applied Sciences*, vol. 12, no. 15, p. 7860, Aug. 2022.
- [38] L. Debschütz, A. Seefried, T. Westermeier, *et al.*, "Experimental investigation of fuel slosh in a generic fighter wing tank configuration", in *33rd Congress of the International Council of the Aeronautical Sciences, ICAS 2022*, Stockholm, Sweden, Sep. 2022.
- [39] J. Hall, T. Rendall, C. Allen, *et al.*, "A multi-physics computational model of fuel sloshing effects on aeroelastic behaviour", *Journal of Fluids and Structures*, vol. 56, pp. 11–32, Jul. 2015, X.
- [40] D. J. Inman, *Engineering vibration*. Prentice Hall Englewood Cliffs, NJ, 2014, vol. 4.
- [41] P. Avitabile, *Modal Testing: A Practitioner's Guide*, 2nd. Wiley, 2017.
- [42] K. Ahlin and A. Brandt, *Experimental Modal Analysis in Practice*. Saven EduTech AB, 2001.
- [43] B. Cauberghe, "Applied frequency-domain system identification in the field of experimental and operational modal analysis", Ph.D. dissertation, Vrije Universiteit Brussel, 2004.

## BIBLIOGRAPHY

- [44] D. Borglund and D. Eller, *Aeroelasticity of Slender Wing Structures in Low-Speed Airflow*. KTH, 2016, TRITA-AVE 2016:78.
- [45] R. L. Bisplinghoff, H. Ashley, and R. L. Halfman, *Aeroelasticity*. Dover Publications Inc, 2013.
- [46] P. Back and U. Ringertz, “Convergence of methods for nonlinear eigenvalue problems”, *AIAA journal*, vol. 35, no. 6, pp. 1084–1087, 1997.
- [47] T. Ye, D. Pan, C. Huang, *et al.*, “Smoothed particle hydrodynamics (sph) for complex fluid flows: Recent developments in methodology and applications”, *Physics of Fluids*, vol. 31, no. 1, 2019.

## About the use of generative AI

The author has not used generative AI tools in the writing of the comprehensive summary. Grammar correction and spell-checking tools built into the word editor (Overleaf) has been used to improve readability.

I take full responsibility for the content of the comprehensive summary of the thesis.



# Appended papers

